J. exp. Biol. 139, 233–252 (1988)
Printed in Great Britain © The Company of Biologists Limited 1988

QUASIELASTIC LASER LIGHT SCATTERING AND LASER DOPPLER ELECTROPHORESIS AS PROBES OF SYNAPTIC AND SECRETORY TERMINAL FUNCTION

By DAVID B. SATTELLE

AFRC Unit of Insect Neurophysiology and Pharmacology, Department of Zoology, University of Cambridge, Downing Street, Cambridge CB2 3EJ, UK

Summary

The intensity fluctuations of scattered laser light provide a rapid, nondestructive probe of hydrodynamic size and polydispersity of nerve-ending subcellular particles. This method yields information on diffusive and directed motion of secretory granules and synaptic vesicles. It also enables accurate measurements of surface charge properties of isolated granules and plasma membranes. Recently, a fast, total intensity light-scattering change, sensitive to many of the factors that influence secretion, has been detected in neurosecretory terminals. Here a slower, but equally reversible, light-scattering change is detected using an intact invertebrate neurosecretory organ. Scattering at rest is dominated by particles of diameter similar to that of secretory vesicles detected in electron micrographs of the same tissue. Simultaneous release and light-scattering observations demonstrate an increase in the proportion of total scatter derived from mobile as opposed to fixed components, with no change in mean particle diameter. Since the major changes in intensity fluctuations are detected during the declining phase of the release of secretory product, they may represent longer term reorganization of terminals following intense secretory activity.

As a prelude to dissecting the origin of the fast light-scattering changes, the hydrodynamic properties of secretosomes and purified secretory granules from mouse neurohypophysis have been characterized. In this way, size, dispersity and aggregation can be followed, and subpopulations can be characterized. Application of an electric field to various subcellular fractions enables measurement of electrophoretic mobility, and hence calculation of surface-charge properties of granules and plasma membranes. The effects of divalent cations on granule surface charge *in vitro* indicate that surface-charge neutralization is not a calcium-specific event in exocytosis. The possibility that some of the light-scattering signal reflects dynamic changes in cytoskeletal components of the secretory terminal is examined.

Introduction

Interaction of light with living cells, subcellular particles and macromolecules has provided extensive information relating to their function. Light scattering,

Key words: laser, light scattering, secretion, nerve terminal.

absorption, fluorescence, rotation, reflection and refraction provide details of shape, size, and motion of macromolecules and subcellular particles. Here, the applications of laser light-scattering techniques to the study of secretion are examined. In such experiments, coherent radiation from a laser source is employed to probe the dynamics of a system of scatterers. Diffusive and directed motion of subcellular particles about the size of secretory and synaptic vesicles can be detected (see Chen, Chu & Nossal, 1981; Sattelle, Lee & Ware, 1982). When coherent, monochromatic light from a laser source illuminates the sample, the light scattered at a particular angle (θ) contains information on the speed and trajectory of the scattering centres. A screen placed in the far field detects a speckle pattern due to interference between light scattered by different particles (see Fig. 1A). As the scatterers move, the intensity of the light at a single point will vary as the phase differences change. Thus the characteristics of the motion under investigation are reflected in the time variation of a single speckle. Changes in a single speckle (or at most a few) are detected by placing pinholes in front of the photomultiplier, thereby defining a single coherence area. Laser light scattering therefore offers a noninvasive probe with the spatial and temporal resolution to investigate particle motion in synaptic and neurosecretory nerve terminals.

Two main experimental approaches have been employed in laser light-scattering studies of secretory dynamics. These are illustrated in Fig. 2. In the first of these, quasielastic laser light scattering (QELS) provides a noninvasive probe of granule dynamics. The relationship governing the frequency change ($\Delta\omega$) of light scattered by a particle moving with a velocity v is the Doppler equation:

$$\Delta\omega = \mathbf{K}\mathrm{v}\,, \tag{1}$$

where $\mathbf{K}$ is the scattering vector of magnitude $(4\pi\mathrm{nv}/\lambda)\sin\frac{\theta}{2}$, where λ is wavelength and n is refractive index. Thus the single frequency shift produced by particles moving with a unique velocity is given by:

$$\Delta\omega = 2\pi\Delta\mathrm{f} = \frac{4\pi\mathrm{nv}}{\lambda}\sin\frac{\theta}{2}\cos\alpha\,, \tag{2}$$

where Δf is the Doppler frequency in the photocurrent power spectrum and the angle between the velocity vector and the scattering vector is α. If several particles, each with a different velocity, act as scatterers, then the spectrum of the

Fig. 1. (A) Speckle pattern derived from a laser light-scattering experiment. For nonmotile scatterers, a stationary pattern is detected. Moving scatterers give rise to 'twinkling', so that a detector placed in the far field observes fluctuations with time of the scattered intensity that reflect the motion of the scattering centres. (B–E) Secretory granules and secretosomes viewed with a Zeiss Axiomat using differential interference optics. (B,D) Constrast features of the video-camera are used to visualize structures below the resolution of the light microscope. (C,E) Colour representation of grey levels; pink representing lighter images. (B,C) Secretory granules purified from mouse neurohypophysis. (D,E) Secretosomes prepared from mouse neurohypophysis. Scale bar, 5·0 μm.

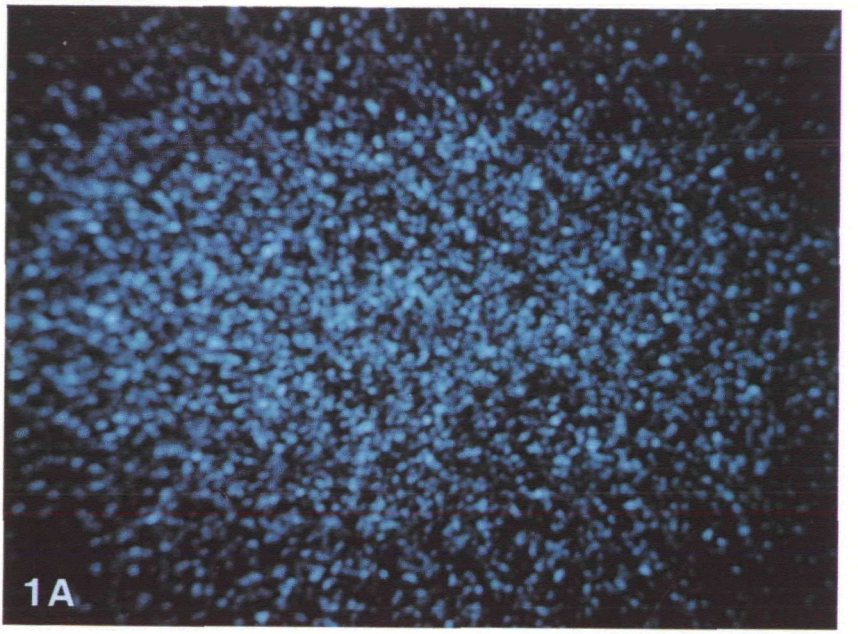
1A


B

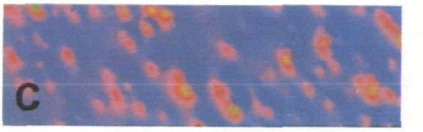
C

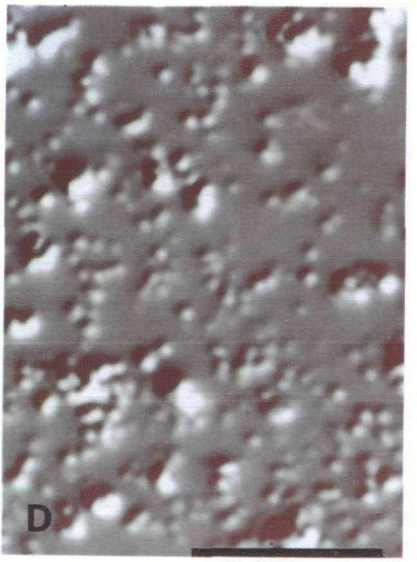
D


E

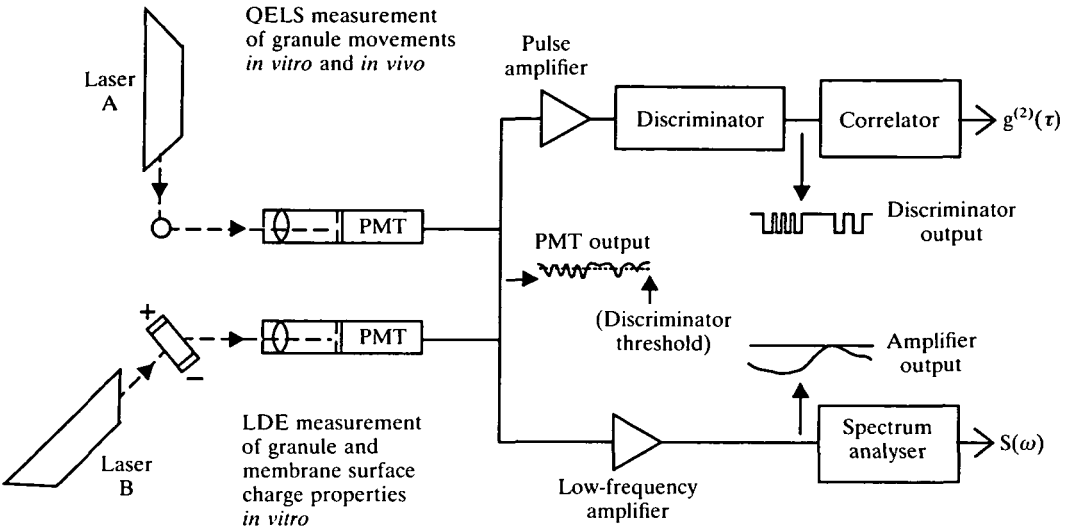

Fig. 2. Schematic representation of experiments designed to monitor secretory granule movements *in vitro* and *in vivo*. Laser A illuminates suspended secretory granules or isolated nerve terminals. Light scattered at a given angle is focused on to the photomultiplier (PMT). This configuration permits quasielastic laser light-scattering (QELS) measurements. Laser B illuminates an electrophoresis cell. Movements of membrane-bound particles subjected to an electric field are detected. Scattered light is focused onto the surface of the photomultiplier. In this way laser Doppler electrophoresis (LDE) measurements of membrane surface charge properties are obtained from secretory granules and plasma membranes.

scattered light will contain all the appropriate Doppler frequencies. In the case of Brownian motion, particles do not maintain a steady velocity, leading to a broadened spectrum centred on the original laser frequency (ω_0), the degree of broadening being related to the diffusion coefficient of the species of particle involved. In this case the frequency spectrum, $S(\omega)$, has a Lorentzian form (see Fig. 3), with a half-width at half-height Γ, where

$$\Gamma = DK^2 . \tag{3}$$

The diffusion coefficient (D) is related to the hydrodynamic particle radius (r) and the viscosity (η) of the suspending fluid by the Stokes–Einstein equation:

$$D = \frac{k_B T}{6\pi\eta r} , \tag{4}$$

where k_B is the Boltzmann constant, and T is the absolute temperature. By monitoring either the power spectrum of scattered laser light (or its inverse Fourier transform, the autocorrelation function of intensity fluctuations with time), simultaneous measurements of diffusion coefficient and total scattered

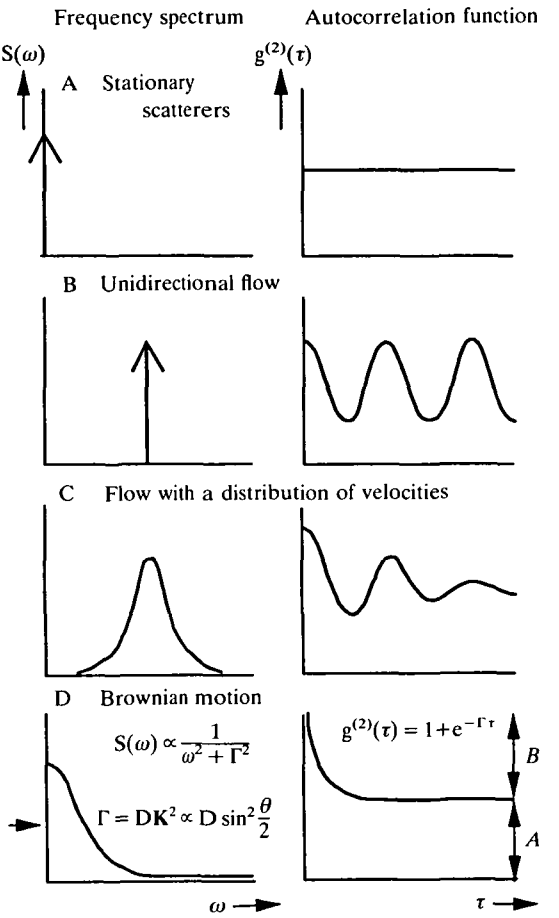

Fig. 3. Laser light-scattering spectra and autocorrelation functions predicted for a diversity of particle motions. Each autocorrelation function is the inverse Fourier transform of the corresponding spectrum.

intensity can be obtained. In this way, granule swelling, aggregation and lysis can be detected *in vitro* (Fig. 4).

Changes in cytoplasmic viscosity, and the proportion of scatterers that are free to diffuse, compared with those that are stationary or tethered (B/A ratio, see Fig. 3D), can be estimated.

In laser Doppler electrophoresis (LDE) experiments (see Fig. 2), the scattering centres are illuminated by a laser whilst being subjected to an electric field. As in the case of QELS the scattered light is detected by a photomultiplier. The electrophoretic velocity of the scattering particles is determined by measuring the Doppler shift in the frequency of scattered light. First described by Ware & Flygare (1971), the technique has been applied to the study of macromolecules, cells and subcellular particles. In such experiments, diffusion is superimposed on directed motion, so the spectrum will be centred on the Doppler-shifted frequency

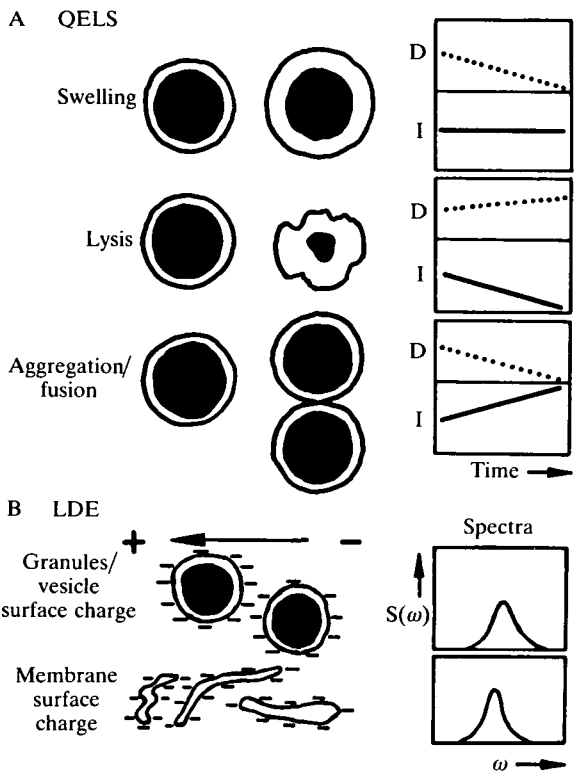

Fig. 4. Schematic representation of some of the properties of secretory vesicles that can be detected in quasielastic laser light-scattering (QELS) and laser Doppler electrophoresis (LDE) experiments. D, diffusion coefficient; I, scattered intensity.

($\omega_0+\Delta\omega$), and broadened by diffusion (in the case of macromolecules) and electrophoretic heterogeneity (in the case of cells and subcellular particles).

Signal processing of the photomultiplier output is normally pursued in two ways depending on the display required. The output of the photomultiplier can be described in terms of spectra or autocorrelation functions (Fig. 2). In the frequency domain, the simplest scheme is to dispatch the photomultiplier output *via* a narrow-bandpass filter to a spectrum analyser. Before the emergence of real-time spectrum analysis, this was a major limitation. In the time domain, photocount autocorrelation is an effective, precise method. Photocount pulses are passed to an amplifier discriminator, and the output fed to a correlator. The intensity second-order autocorrelation function $g^{(2)}(\tau)$ compares the scattered intensity, recorded as photocounts n(t) at a given time t, with that at a later time $n(t+\tau)$ averaged for all values of τ. Thus, the normalized correlation function is given by:

$$g^{(2)}(\tau) = N\frac{\Sigma n(t)n(t+\tau)}{[\Sigma n(t)]^2}. \qquad (5)$$

The mean decay rate (τ_0) of the autocorrelation function for spheres undergoing Brownian motion is related to the spectral half-width (Γ) by the relationship:

$$\Gamma = \frac{1}{\tau_0}. \tag{6}$$

The correlation function is sensitive to faster processes, but both spectrum analysis and photocount autocorrelation are equally applicable to events on the biological timescale. Experimental chambers employed in QELS and LDE experiments are illustrated in Fig. 5.

Synaptic nerve terminals

Shaw & Newby (1972) first attempted direct measurements of synaptic vesicle motion *in vivo* using quasielastic laser light scattering (QELS). The preparation chosen was the neuropile of a locust ganglion, a tissue rich in synaptic, particularly cholinergic (Breer & Sattelle, 1987), nerve terminals. A reversible increase in intensity fluctuations was detected in response to potassium depolarization. Experiments on the same tissue showed that the enhanced amplitude of the spectrum was the same at all frequencies in the range 6·3–150 Hz, and the form of the spectra recorded from depolarized ganglia remained essentially unchanged (Piddington & Sattelle, 1975; Sattelle & Piddington, 1975). For a cytoplasmic viscosity of 0·006 Pa·s, the bulk of the scattering could be attributed to particles 50–500 nm in diameter. Attempts to observe optical fluctuations in response to electrical stimulation of invertebrate neuropile have not yielded consistent results. However, Moore, Tufts & Soroka (1975) detected increases in spectral amplitude during electrical depolarization of the squid (*Loligo pealei*) giant axon, though the origin of these signals is unknown.

Using squid (*Loligo pealei*) optic lobes as a source of tissue, QELS has been employed to characterize the size and dispersity of synaptosomes and purified synaptic vesicles. Synaptosomal fractions were highly polydisperse ($\mu_2/\bar{\Gamma}^2 = 0{\cdot}5$), and the mean diameter ($\bar{d}$) ranged from 0·5 to 2·0 μm.

Size distribution histograms yielded two major components – smaller particles ($\bar{d} \approx 300$–700 nm) and a larger group of particles ($\bar{d} \approx 1500$–5000 nm). The heterogeneity of the synaptosomal particles detected in solution (Fig. 6) is in agreement with published data obtained using electron microscopy (Haghighat, Cohen & Pappas, 1984). These authors describe five subtypes of nerve endings in the intact optic lobe of *Loligo*, corresponding to five distinct types of terminal seen in the synaptosome fraction. Two of these categories, which probably correspond to different classes of photoreceptor nerve endings in the cortex of the optic lobe, are made up of terminals often much larger than 1 μm in diameter. The other three distinct types of terminal seen by electron microscopy are smaller, and correspond to the nerve endings seen in the medulla region (Haghighat *et al.* 1984). The simplest explanation for the bimodal distribution of particle sizes seen in QELS experiments is that they represent the two size categories of nerve terminals noted

in ultrastructural studies. In this context it is of interest to note that Redburn & Thomas (1979) isolated two morphologically distinct synaptosomal fractions from rabbit retina. One of these was enriched in relatively large diameter photoreceptor cell synaptosomes, whereas the other contained smaller synaptosomes derived from conventional-sized nerve endings from the inner plexiform layer.

Veratridine depolarizes nerve terminals releasing neurotransmitter (Minchin, 1980). Depolarization by veratridine ($1{\cdot}0\times10^{-4}$ mol l^{-1}) did not result in a detectable change in the total scattered intensity or hydrodynamic size of synaptosomes isolated from the squid (Sattelle, Langley, Obaid & Salzberg, 1987). The absence of any striking change in either total scattered intensity or mean particle size during veratridine-induced depolarization does not preclude the existence of a transient intensity change of the kind recorded from intact vertebrate neurosecretory nerve endings (see Salzberg, Obaid, Gainer & Senseman, 1983; Salzberg, Obaid & Gainer, 1985). These authors have detected a rapid change in total scattered intensity, probably representing an increase in large-angle scattering, accompanying calcium-sensitive secretory release in nerve terminals. Further experiments are needed on a shorter timescale to test whether such light-scattering changes can be reproduced in isolated nerve endings.

Purified synaptic vesicle fractions also yielded complex particle size distribution data. A component with a mean diameter in the range 150–250 nm was detected, though a smaller particle ($\bar{d} \approx 40$–110 nm) dominated the scattering signal (Fig. 6). This smaller particle closely resembles in size the electron-lucent vesicles seen in the majority of squid optic lobe nerve terminals when examined by electron microscopy. Osmotically induced shrinkage and swelling of the synaptosomes was detected by means of QELS (Sattelle *et al.* 1987).

Using laser Doppler electrophoresis, Siegel & Ware (1980) measured electrophoretic mobilities of synaptic vesicles and synaptosomal plasma membranes from guinea pig cerebral cortex. The electrophoretic mobility of synaptic vesicles is slightly greater than that of synaptosomal plasma membranes. Calcium and magnesium reduced the mobility of both types of particle to the same extent at physiologically relevant concentrations (0–1·0 mmol l^{-1}) and near-physiological ionic strength. At concentrations of 2·0 mmol l^{-1} and higher, calcium reduced the mobility of synaptic vesicles more effectively than magnesium. A similar, but smaller, effect was observed in the case of synaptosomal membranes. The similarity of synaptic vesicle and synaptosomal plasma membrane electrophoretic mobilities precludes *in vitro* studies on vesicle–membrane interactions.

Studies on synaptic vesicles, synaptosomes and neuropilar regions rich in synaptic terminals have shown that an increase in intensity fluctuations of scattered light accompanies depolarization of synaptic terminals. Subpopulations of synaptic vesicles and synaptosomes have been detected by QELS. Whereas physiological calcium concentrations influence the electrokinetic properties of synaptosomal membranes, LDE experiments show that calcium and magnesium are equally effective in reducing the surface charge on synaptic vesicles. Though screening by divalent cations of membrane surface charge will promote vesicle–

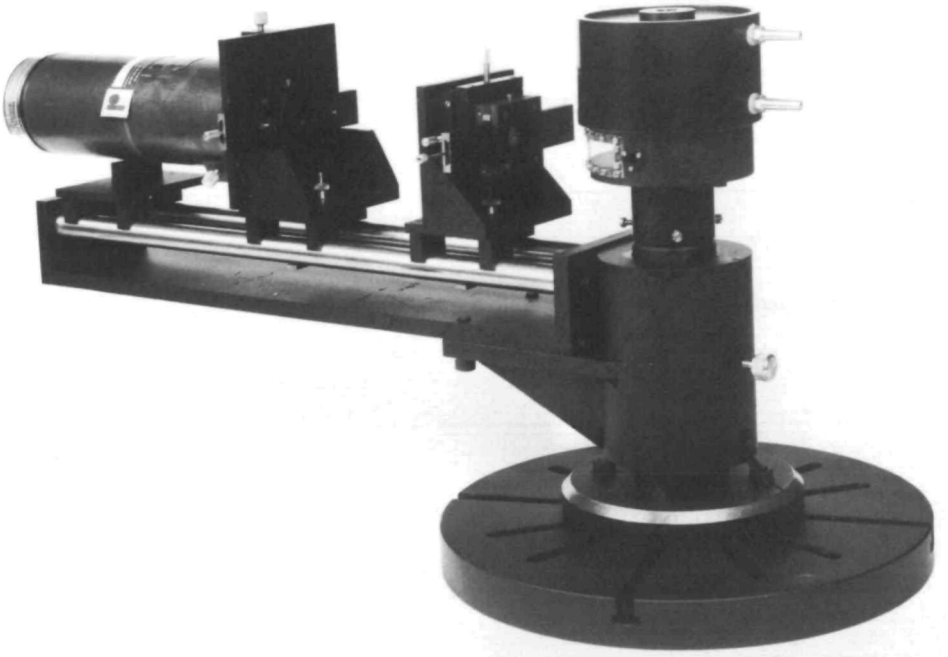

5A

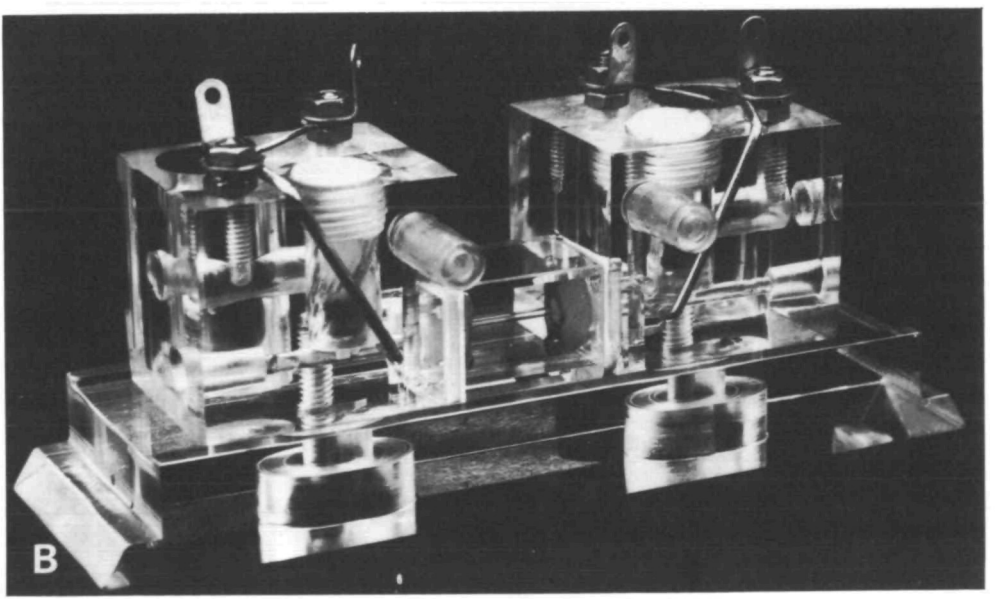

membrane interactions, it is clearly not the calcium-specific step in synaptic vesicle release.

Neurosecretory nerve terminals

Laser light scattering has emerged as a sensitive probe of secretory granule hydrodynamic properties. The size, dispersity and calcium-induced aggregation of adrenergic (chromaffin) secretory vesicles has been studied by means of laser light scattering. All such granule preparations were polydisperse, as judged by the departure of the intensity autocorrelation function from a single exponential. Granules purified by differential centrifugation in $0{\cdot}3\,mol\,l^{-1}$ buffered sucrose were less polydisperse than those prepared using a sucrose–Ficoll–D_2O mixture. The following mean diameters were computed from $D_{20,w}$: 400 ± 33 nm for sucrose granules in $0{\cdot}3\,mol\,l^{-1}$ sucrose and 170 ± 23 nm for sucrose granules in $1{\cdot}6\,mol\,l^{-1}$ sucrose (Sattelle, Green, Langley & Westhead, 1976; Green, Westhead, Langley & Sattelle, 1978).

The same authors detected both swelling and aggregation of granules by noting changes in diffusion coefficient (D) and scattered intensity (I). Granules resuspended in hyposmotic solutions ($0{\cdot}15\,mol\,l^{-1}$ NaCl or KCl) showed a rapid decrease in D accompanied by a steady decline in I, indicating swelling of the granules and loss of contents. Calcium-ion-induced aggregation of granules was detected at a threshold of $2–10\,mmol\,l^{-1}$ calcium as an increase in I and a corresponding decrease in D.

Calcium has been established as a major signal for secretion from adrenal chromaffin cells (Baker & Knight, 1981). Siegel, Ware, Green & Westhead (1978) performed LDE measurements on chromaffin granules, with particular reference to the role of divalent cations in modifying surface charge properties. Calcium and magnesium were equally effective in reducing the electrophoretic mobilities. The results are consistent with the observations of Morris & Schober (1977) who measured calcium and magnesium binding to chromaffin granules and the resultant aggregation under conditions of low ionic strength. The equivalence of calcium and magnesium in reducing the surface charge of chromaffin granules is evidence that the specific role of calcium in triggering neurosecretory release is due to effects other than the ability of calcium to reduce the electrostatic repulsion between charged membranes.

Fig. 5. (A) The spectrometer used for quasielastic laser light-scattering (QELS) experiments on purified synaptic vesicles, secretory granules, synaptosomes and secretosomes. Samples are examined in a temperature-controlled housing. The spectrometer 'arm' includes a rotatable optical bench bearing adjustable aperture, pinhole and lenses, and directs light scattered at a selected angle onto the photomultiplier tube. (B) Electrophoresis cell used for laser Doppler electrophoresis (LDE) measurements on secretory granules. The incident laser beam is directed onto the sample material in the narrow horizontal glass tube. The sample is subjected to an electric field *via* the Ag/AgCl electrodes, and the scattered light is directed onto a photomultiplier.

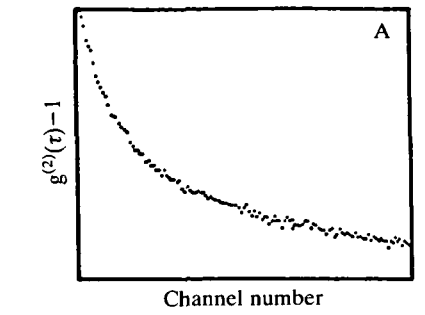

	Synaptosomes	Synaptic vesicles
Moments analysis		
$\mu_2/\bar{\Gamma}^2$	0·57	0·35
$\bar{d}$l	997 nm	97 nm
SDP analysis		
d_1	292 nm (36 %)	54 nm (38 %)
d_2	3600 nm (64 %)	228 nm (62 %)

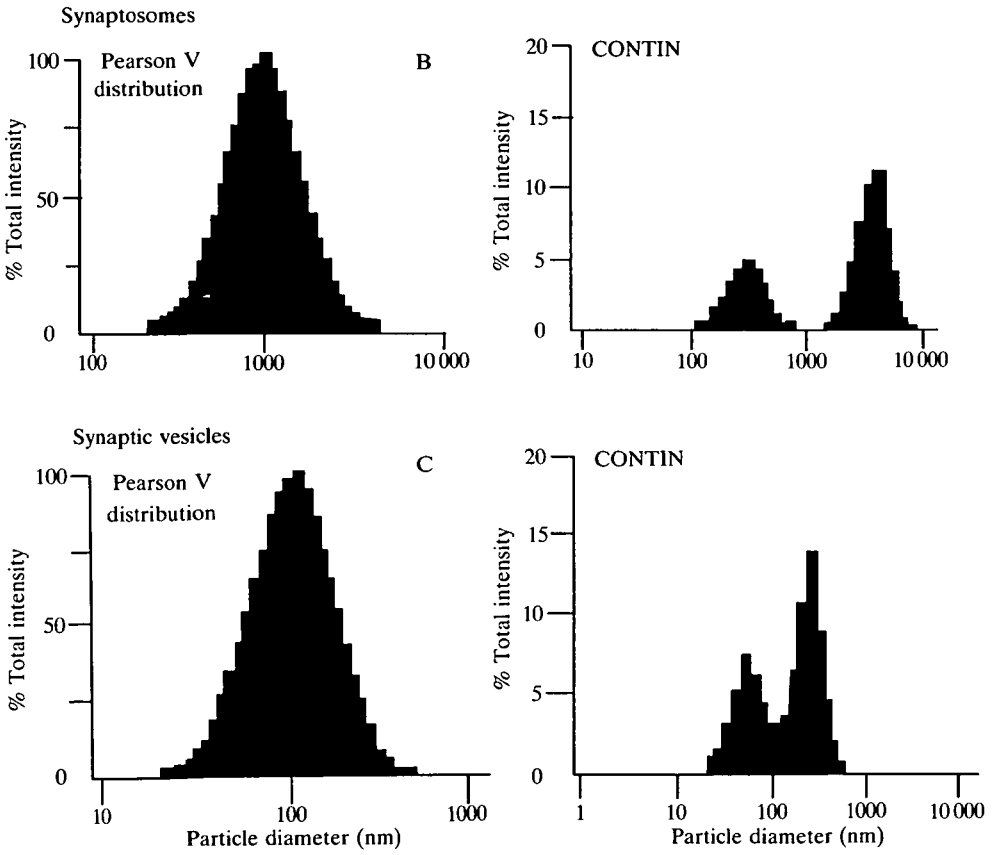

Fig. 6. (A) Intensity autocorrelation function derived from squid (*Loligo pealei*) optic lobe synaptosomes in artificial sea water plotted as $g^{(2)}(\tau)-1$ against channel number. Such data are used for particle size distribution analysis. (B) Particle size distribution of crude synaptosomes is estimated by fitting data to the Pearson V distribution (McCally & Bargeron, 1977); particle size distribution is also determined using the CONTIN programme developed at the European Molecular Biology Laboratory in Heidelberg, Germany for the constrained regularization of linear equations (see Provencher, 1982*a*,*b*). Two populations of secretosomes are resolved. (C) Squid (*Loligo pealei*) optic lobe synaptic vesicles are suspended in axoplasm buffer and data are analysed as for synaptosomes. Two populations of vesicles are resolved. Polydispersity ($\mu_2/\bar{\Gamma}^2$) is determined from the decay rate (τ_0) of $g^{(2)}(\tau)-1$ by moments analysis. The average hydrodynamic diameter ($\bar{d}$) is estimated from the Stokes–Einstein equation using the experimentally determined diffusion coefficient.

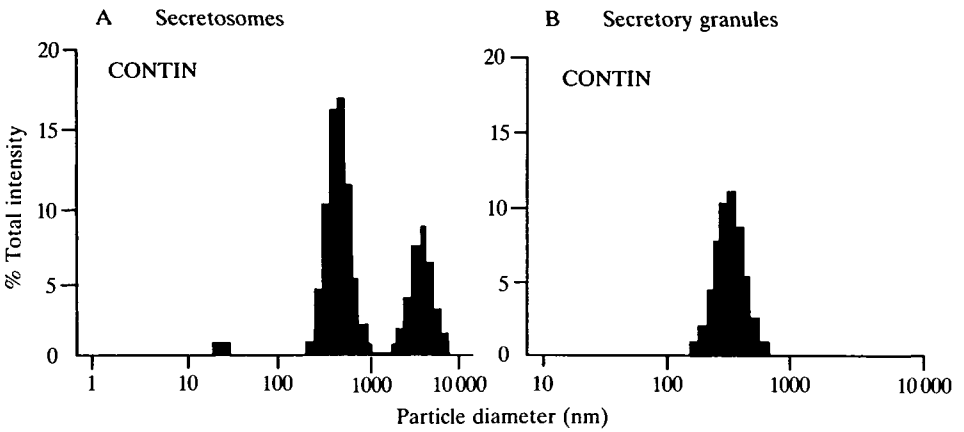

Fig. 7. Particle size distribution obtained by applying the CONTIN analysis programme to intensity autocorrelation functions derived from light scattered (A) by isolated neurosecretory nerve endings (secretosomes) and (B) granules purified from mouse neurohypophysis. Isolated granules are suspended in filtered sucrose buffer.

The size and polydispersity of insulin-containing granules isolated from rat pancreatic islets have been characterized by QELS (Matthews *et al.* 1982). Granules exhibited a mean diameter of 342 nm, and a buoyant density of 1·104. The same method was used by McKay & Matthews (1982) to investigate the effects of a pancreatic acinar cytoplasmic factor on zymogen granule interactions *in vitro*. This trypsin-sensitive protein inhibits the potassium-induced granule aggregation by >75 %. Recently, this work has been extended using purified rat pancreatic zymogen granules *in vitro* (Rogers, Matthews & McKay, 1987). Isolated granules in isotonic sucrose (pH 6·0) maintained a mean diameter of 1225 ± 18 nm. A soluble protein fraction separated from the pancreatic acinar cell cytosol reduced the mean diameter and polydispersity index of zymogen granules suspended in isotonic sucrose. This protein also inhibited cation-induced aggregation and stabilized granules to solubilization resulting from either an increase in pH (> 7·0) or exposure to media of high ionic strength. The inhibitory effects of this protein were not mimicked by bovine serum albumin, the calcium-binding proteins calmodulin and troponin C, or by the highly negatively charged polymer, polyglutamate. Thus, QELS has provided a sensitive assay for aggregation inhibitors, and may serve to reveal other candidate cytoplasmic modulatory factors with possible roles in regulating secretory discharge.

Secretosomes isolated from mouse neurohypophysis have been examined by QELS techniques (Fig. 7). Preliminary particle size distributions indicate the presence of a wide range of particle sizes (D. B. Sattelle, A. L. Obaid, J. Russell & B. M. Salzberg, unpublished observations). Purified secretory granules from mouse neurohypophysis are polydisperse, but both moments analysis and particle size distribution analysis (Fig. 7) reveal a monomodal distribution of scatterers. These isolated granules have been used to investigate calcium-induced aggre-

gation (Fig. 8). As in the case of chromaffin granules, aggregation is readily detected by following simultaneous changes in D and I. Laser Doppler electrophoresis applied to mouse neurohypophysis granules reveals that electrophoretic mobility is reduced almost equally effectively by calcium (Fig. 9) and magnesium.

The recent discovery that in the neurohypophysis the secretory event is accompanied by large and rapid changes in light scattering (see Salzberg & Obaid, 1988, for a review) has prompted an initial series of QELS experiments on this neurosecretory organ. Light scattered at a variety of angles from isolated mouse neurohypophysis was investigated by QELS. A monotonically decaying intensity autocorrelation function was obtained which was not fitted by a single exponential, indicating a distribution of scattering species (D. B. Sattelle, A. L. Obaid & B. M. Salzberg, unpublished observations). Moments analysis was employed to obtain a mean decay rate $\left(\frac{1}{\Gamma}\right)$, from which values of diffusion coefficient and hydrodynamic radius were obtained. The bulk of the scattering derived from particles 0·5–2·0 μm in diameter. Nevertheless, distinct curvature of the intensity autocorrelation function at shorter sample times indicated that some scattering was also derived from particles about the size of secretory vesicles. A stimulation regime that successfully generated a light-scattering change (detected by microscopy using a.c. coupling of the optical signal) was applied to mouse neurohypophysis. No change in decay rate of the autocorrelation function was detected either at short sample times or at longer sample times (500 ms). No consistent change was detected in B/A (the ratio of moving to stationary scatterers). Although there are several examples of slow light-scattering changes monitored by QELS from neurosecretory tissues (following, for example, potassium stimulation), the rapid light-

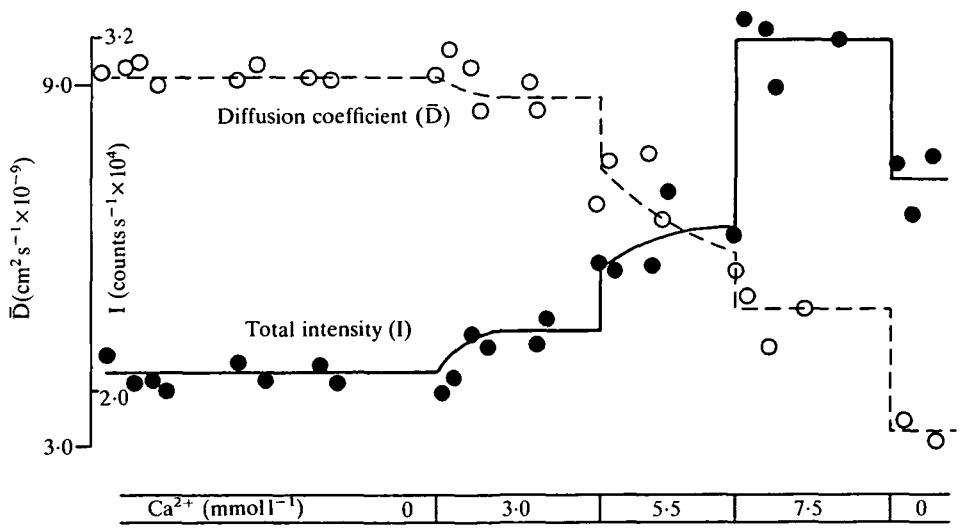

Fig. 8. Calcium-induced aggregation of mouse neurohypophysis granules. Changes in mean diffusion coefficient ($\bar{D}$) and total scattered intensity (I) are followed as the calcium concentration is increased.

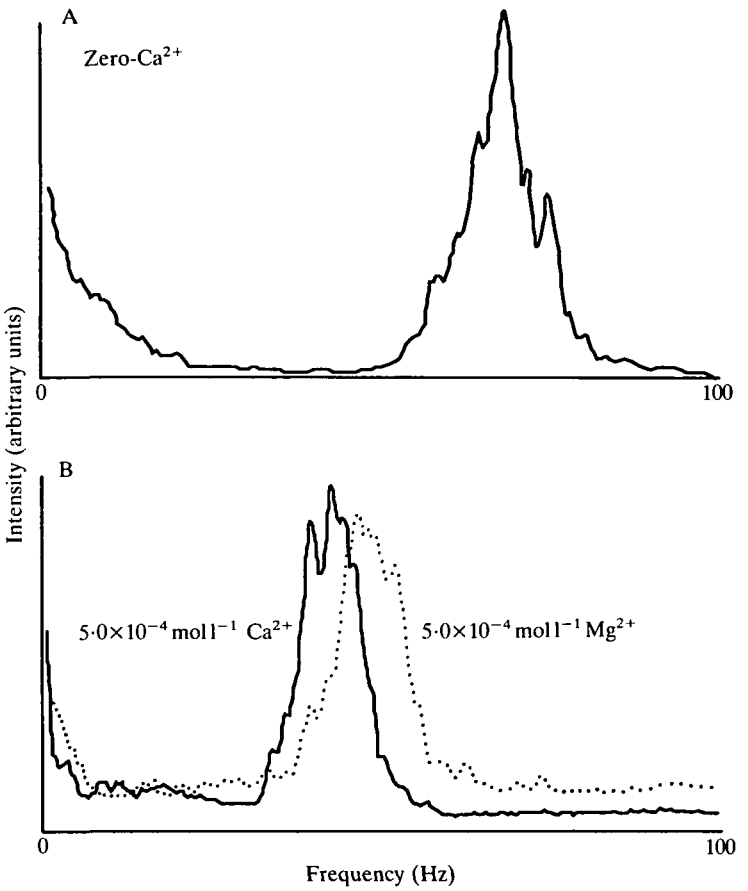

Fig. 9. Electrophoretic spectra derived from secretory granules prepared from mouse neurohypophysis. (A) Granules suspended in zero-calcium buffer; (B) granules from the same preparation suspended in buffer containing either calcium ($5{\cdot}0\times10^{-4}$ mol l^{-1}) or magnesium ($5{\cdot}0\times10^{-4}$ mol l^{-1}).

scattering changes that take place on the timescale of secretory release appear to constitute a small fraction of the total scattered intensity detected in the QELS experiments performed to date, in which several seconds are required to accumulate data for an autocorrelation function. It will be of considerable interest in future to pursue the collection of intensity autocorrelation data over progressively shorter periods, ideally on a subsecond timescale.

Combined laser light scattering and release studies

Laser light scattering has been used to investigate particle motion in the isolated pericardial organ of the lobster (*Homarus americanus*) (Sattelle, Green & Langley, 1975; Englert & Edwards, 1977). These invertebrate organs contain numerous peripherally located neurosecretory cell processes. An experimental

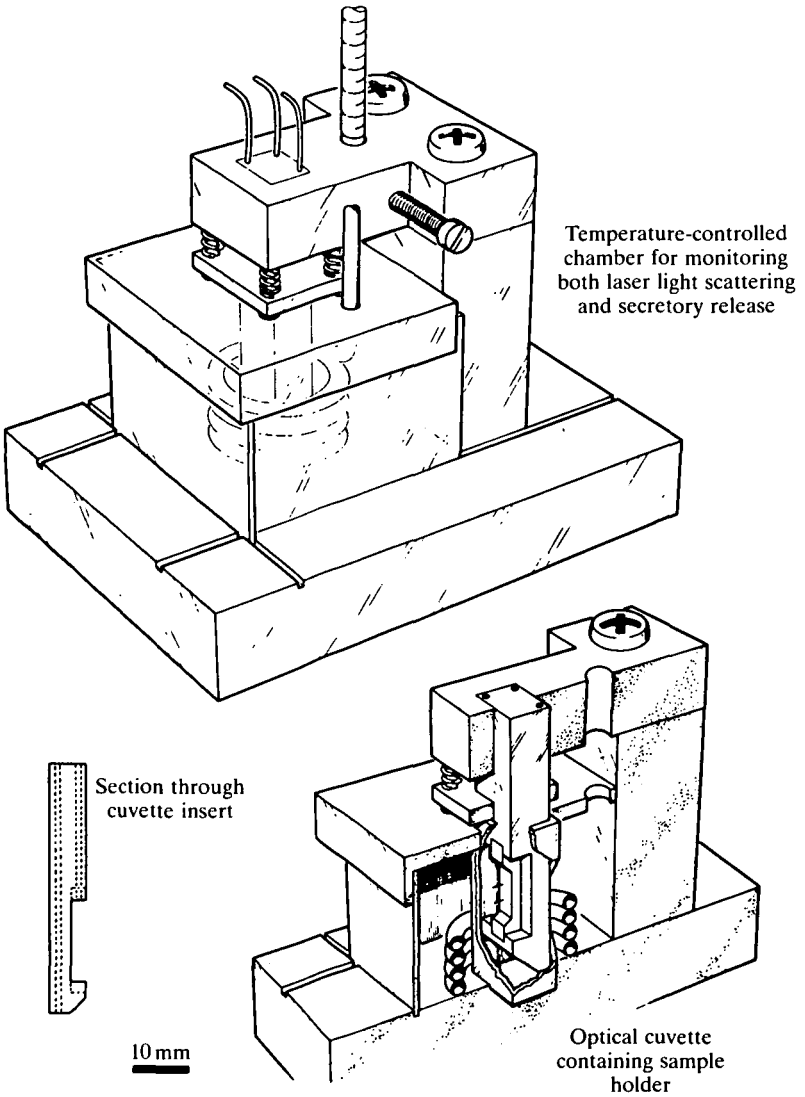

Fig. 10. Experimental chamber for simultaneous recording of laser light-scattering signals and secretory release from an invertebrate neurosecretory organ. The temperature-controlled chamber permits rapid removal and replacement of the cuvette contents for analysis of released radiolabel.

chamber has been devised (Fig. 10), in which the tissue is mounted under saline in a water-cooled (14–16°C) optical glass cuvette. The chamber was flushed with fresh saline at regular intervals. Scattered laser light from a 100 μm diameter circular area of the surface of the pericardial organ was detected by a photomultiplier placed at 90° to the attenuated incident He–Ne laser beam. As shown in Fig. 11, the autocorrelation function has a monotonically decaying, time-dependent component which derives from moving scatterers, and a time-independent

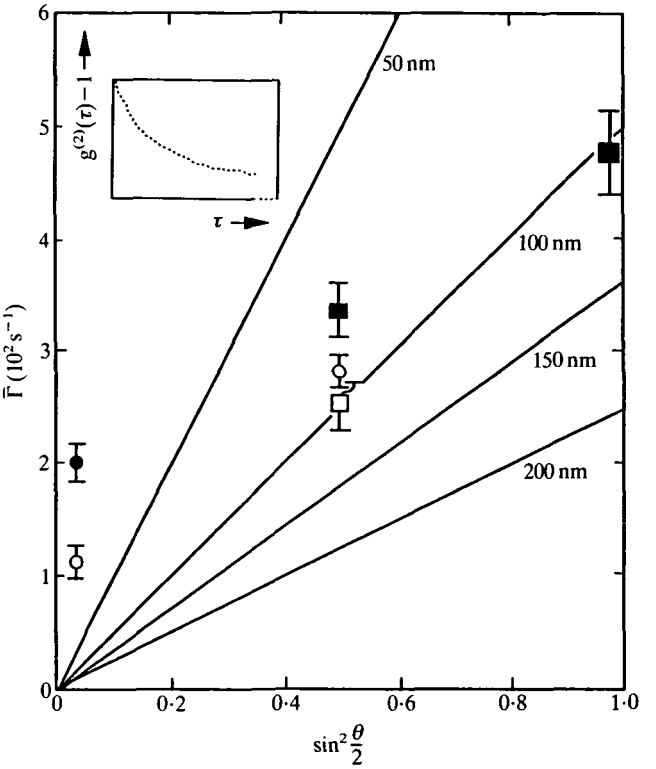

Fig. 11. Plot of the initial decay rate ($\bar{\Gamma}$) of the intensity autocorrelation function as a function of the scattering angle θ. For particles undergoing diffusive motion in cytoplasm, a linear relationship is predicted between $\bar{\Gamma}$ and $\sin^2\frac{\theta}{2}$. Straight lines show the relationships predicted for particles of various diameters. Inset is an intensity autocorrelation function derived from laser light scattered by the neurosecretory pericardial organ of the lobster (*Homarus americanus*). Each channel represents 20 μs.

component originating from stationary scattering structures. The bulk of the motile scatterers appeared to have diameters in the size range 100–400 nm. From the complex angular dependence of the decay rate of the autocorrelation function, it is evident that a range of scatterers contribute to the signal, but the predominant scattering particles are about the size of neurosecretory vesicles.

Pericardial organs were preloaded with [^{3}H]tyramine, which in these arthropod structures is primarily released as octopamine (Sullivan, Friend & Barker, 1974). One major change was noted in the correlation function when neurosecretory release was stimulated by increasing the potassium level in normal saline from 16 to 100 mmol l^{-1}. During exposure to high potassium there was a reversible transient increase in the amplitude of the correlation function derived from moving scatterers relative to that derived from stationary scatterers. In 11 out of 14 such responses from eight pericardial organs, the amplitude increase appears to be

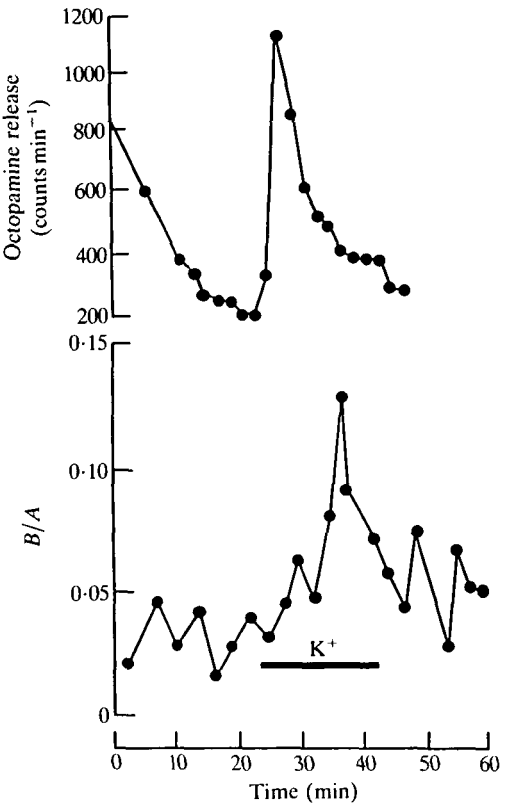

Fig. 12. Plot of octopamine release with time from an isolated pericardial organ preloaded with [^{3}H]tyramine, and depolarized by exposure to a high (100 mmol l^{-1}) potassium saline. The bulk of the label is released as [^{3}H]octopamine. Although no change in the decay rate of the autocorrelation function accompanies the discharge of octopamine, an increase in the total intensity of scattering attributable to moving scatterers is detected. The peak of the light-scattering response coincides with the declining phase of release of neurosecretory material. B/A ratio is defined in Fig. 3 and represents the ratio of mobile to stationary scattering elements.

related to events that follow the main discharge of neurosecretory material (Fig. 12).

In addition to exploiting QELS as a potential probe of the secretory event, Ware and colleagues have explored LDE in this context using mast cells, which are responsible for the secretion of histamine in certain immune responses. The aim of these experiments was to exploit any differences in electrophoretic mobility between granule and plasma membranes as a means of detecting secretion. Fig. 13 shows the effects on electrophoretic mobility distribution of mast cells of immunological stimulation at various levels of dilution of the F(ab')$_2$ fragments which are used to stimulate mast cell secretion. Clearly, stimulation leads to an increased mobility of the secreting population. Controls were performed to show that the observed changes were not due to the effect on the cell surface of

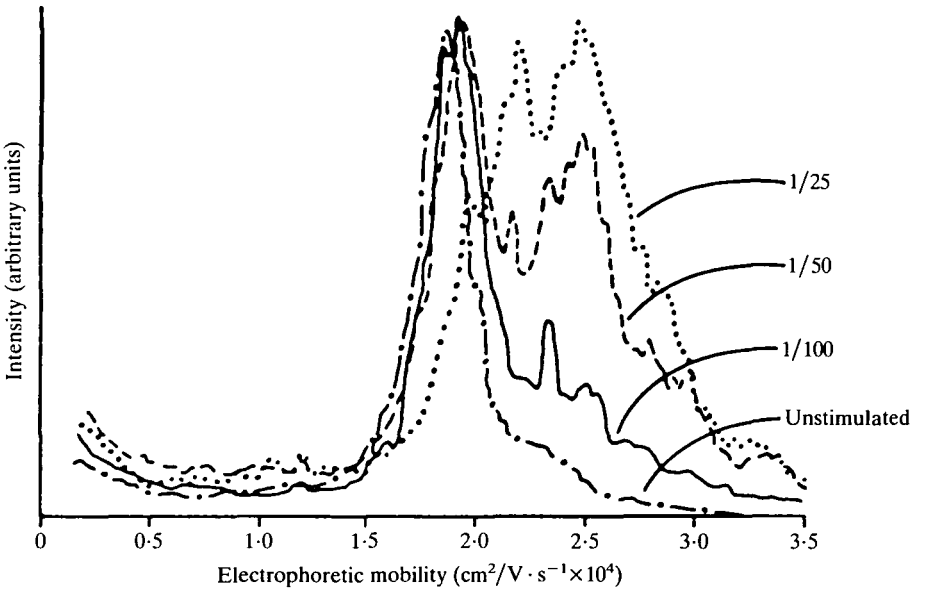

Fig. 13. Effects of immunological activation on rat mast cell electrophoretic mobility distribution are illustrated. The dose–response curve of the activation is indicated by showing LDE spectra of mast cells incubated at 37°C with various dilutions (1/100, 1/50, 1/25) of rabbit anti-rat $F(ab')_2$ antiserum. Apparently exocytotic secretion adds new highly charged membrane to the cell surface, creating a population of cells with substantially higher electrophoretic mobility. From Petty, Ware & Wasserman (1980).

components which may have been secreted as a result of the stimulation. Since the electrophoretic mobility of the vesicles is not that different from values observed for the mast cell, an interpretation of the results based on fusion between granules and plasma membrane demands a high negative surface charge density on the interior of the mast cell vesicles.

Conclusions

Interpretation of total intensity light-scattering changes associated with secretion are discussed in detail elsewhere (Salzberg & Obaid, 1988). These authors review evidence that a component of light-scattering recorded from mouse neurohypophysis terminals and secretory release from the same tissue are sensitive to many of the same external factors. Despite the excellent correlation obtained, the precise step in the sequence of events coupling excitation to secretion remains to be resolved. Here, consideration will be given to possible interpretations of the slower light-scattering signals detected by QELS. Failure to detect a change in the decay rate of the autocorrelation function argues against a volume change as the major contribution to the scattering from secretory terminals. Swelling of nerve terminals has been advanced as a possible interpretation of the QELS changes recorded from depolarized synaptic and secretory terminals (Englert & Edwards,

1977), but these authors have not performed simultaneous release and light-scattering experiments. An increase in the ratio of mobile to stationary scattering elements that follows secretory discharge could be interpreted in terms of depolymerization or disaggregation of some of the nerve-ending cytoskeletal elements, since it is not accompanied by a change in autocorrelation function decay rate. At the sample times employed, cytoskeletal structures would contribute to the time-independent (stationary) component of the autocorrelation function in unstimulated terminals. If the discharge of neurosecretory material is associated with depolymerization, a decrease in the proportion of scattering deriving from stationary relative to mobile scattering elements would be anticipated.

The notion that reorganization of cortical actin filaments is required to allow access of secretory granules to exocytotic sites was advanced by Orci, Gabbay & Malaisse (1972) in studies of pancreatic beta cells. However, direct evidence that actin filament disassembly accompanies the secretory process has only recently been obtained (Cheek & Burgoyne, 1986; Burgoyne & Cheek, 1987). Work on permeabilized cells has shown that agents resulting in disassembly of the F-actin network promote calcium-stimulated secretion (Lelkes, Friedman, Rosenheck & Oplatka, 1986). Perrin & Aunis (1985) advanced a role for fodrin in secretory discharge. On stimulation of secretory cells, the distribution of fodrin changes (Perrin & Aunis, 1985). Though its precise role is still being evaluated, it is of interest to note that antisera to the alpha subunit of brain fodrin partially inhibit calcium-induced secretion from digitonin-permeabilized adrenal chromaffin cells (Perrin, Langley & Aunis, 1987).

Bähler & Greengard (1987) showed recently that synapsin I promotes the formation of actin bundles only in its dephosphorylated form. Since it is known that synapsin I can regulate the availability of synaptic vesicles for exocytosis (Llinas, McGuinness, Sugimori & Greengard, 1985), it is possible that dephosphorylated synapsin I contributes to 'restraining' synaptic vesicles in some way, possibly *via* an actin network. Such a restraint would be removed in response to nerve terminal activation, as a result of phosphorylation of synapsin I by depolarization-activated protein kinases.

Thus, a number of ultrastructural observations and data from permeabilized cells, biochemical and quasielastic laser light-scattering (QELS) studies are consistent with dynamic changes in cytoskeletal components, involving reorganization into smaller assemblies and/or depolymerization as a step in secretion. Undoubtedly, quasielastic laser light scattering and laser Doppler electrophoresis will continue to contribute to *in vitro* studies. Further dissection of dynamic events *in vivo* by these optical methods will be enhanced by (a) collection of intensity autocorrelation functions on the subsecond timescale, and (b) improved spatial definition of the scattering elements, possibly by the use of a laser Doppler microscope.

The author is particularly indebted to Dr B. M. Salzberg and Dr A. L. Obaid

(University of Pennsylvania) in collaboration with whom some of the experiments were performed. Thanks are also due to Dr J. Russell and Dr H. Gainer (NIH) for helpful advice during the course of this work. Dr P. D. Evans (AFRC, Cambridge) kindly participated in the experiments on lobster pericardial organs. Coulter Instruments generously supplied some of the equipment used in this study.

References

BÄHLER, M. & GREENGARD, P. (1987). Synapsin I bundles F-actin in a phosphorylation-dependent manner. *Nature, Lond.* **326**, 704–707.

BAKER, P. F. & KNIGHT, D. E. (1981). Calcium control of exocytosis and endocytosis in bovine adrenal medullary cells. *Phil. Trans. R. Soc. Ser.* B **296**, 83–103.

BREER, H. & SATTELLE, D. B. (1987). Molecular properties and functions of insect acetylcholine receptors. *J. Insect Physiol.* **33**, 771–790.

BURGOYNE, R. D. & CHEEK, T. R. (1987). Reorganisation of peripheral actin filaments as a prelude to exocytosis. *Biosci. Reports* **7**, 281–288.

CHEEK, T. R. & BURGOYNE, R. D. (1986). Nicotine-evoked disassembly of cortical actin filaments in adrenal chromaffin cells. *FEBS Letts* **207**, 110–207.

CHEN, S.-H., CHU, B. & NOSSAL, R. (1981). *Scattering Techniques Applied to Supramolecular and Non-Equilibrium Systems*. New York: Plenum Press. pp. 1–928.

ENGLERT, D. & EDWARDS, C. (1977). Effect of increased potassium concentrations on particle motion within a neurosecretory structure. *Proc. natn. Acad. Sci. U.S.A.* **74**, 5759–5763.

GREEN, D. J., WESTHEAD, E. W., LANGLEY, K. H. & SATTELLE, D. B. (1978). Aggregation and dispersity of isolated chromaffin granules studied by intensity fluctuation spectroscopy. *Biochim. biophys. Acta* **539**, 364–371.

HAGHIGHAT, N., COHEN, R. S. & PAPPAS, G. D. (1984). Fine structure of squid (*Loligo pealeii*) optic lobe synapses. *Neuroscience* **13**, 527–546.

LELKES, P. I., FRIEDMAN, J. E., ROSENHECK, K. & OPLATKA, A. (1986). Destabilization of actin filaments as a requirement for the secretion of catecholamines from permeabilized chromaffin cells. *FEBS Letts* **208**, 357–363.

LLINAS, R., MCGUINNESS, T. L., SUGIMORI, M. & GREENGARD, P. (1985). Intraterminal injection of synapsin I or calcium/calmodulin dependent protein kinase II alters the neurotransmitter release at the squid giant synapse. *Proc. natn. Acad. Sci. U.S.A.* **82**, 3035–3039.

MCCALLY, R. L. & BARGERON, C. B. (1977). Application of intensity correlation spectroscopy to the measurement of continuous distributions of spherical particles. *J. Chem. Phys.* **67**, 3151–3156.

MCKAY, D. B. & MATTHEWS, E. K. (1982). Guinea-pig pancreatic zymogen granule interaction *in vitro*: effects of a cytoplasmic protein. *J. Physiol., Lond.* **330**, 38–39P.

MATTHEWS, E. K., O'CONNOR, M. L. D., MCKAY, D. B., FERGUSON, D. R. & SCHUZ, A. D. (1982). Insulin secretory mechanisms and antidiabetic drug action: an investigation by photon correlation spectroscopy and laser–Doppler electrophoresis. In *Biomedical Applications of Laser Light Scattering* (ed. D. B. Sattelle, W. I. Lee & B. R. Ware), pp. 311–321. Amsterdam: Elsevier Biomedical Press.

MINCHIN, M. C. W. (1980). *Veratrum* alkaloids as transmitter releasing agents. *J. Neurosci. Methods* **2**, 111–112.

MOORE, L. E., TUFTS, M. & SOROKA, M. (1975). Light scattering spectroscopy of the squid axon membrane. *Biochim. biophys. Acta* **382**, 286–294.

MORRIS, S. J. & SCHOBER, R. (1977). Demonstration of binding sites for divalent and trivalent ions on the outer surface of chromaffin granule membranes. *Eur. J. Biochem.* **75**, 1–12.

ORCI, L., GABBAY, K. H. & MALAISSE, W. J. (1972). Pancreatic beta-cell web: its possible role in insulin secretion. *Science* **175**, 1128–1130.

PERRIN, D. & AUNIS, D. (1985). Reorganization of α-fodrin induced by stimulation in secretory cells. *Nature, Lond.* **315**, 589–592.

PERRIN, D., LANGLEY, O. K. & AUNIS, D. (1987). Anti α-fodrin inhibits secretion from permeabilized chromaffin cells. *Nature, Lond.* **326**, 498–501.

PETTY, H. R., WARE, B. R. & WASSERMAN, S. I. (1980). Alterations of the electrophoretic mobility distribution of rat mast cells after immunologic activation. *Biophys. J.* **30**, 41–50.

PIDDINGTON, R. W. & SATTELLE, D. B. (1975). Motion in nerve ganglia detected by light-beating spectroscopy. *Proc. R. Soc.* B **190**, 415–420.

PROVENCHER, S. W. (1982*a*). A constrained regularization method for inverting data represented by linear algebraic or integral equations. *Comput. Phys. Commun.* **27**, 213–227.

PROVENCHER, S. W. (1982*b*). CONTIN – A general purpose constrained regularization program for inverting noisy linear algebraic and integral equations. *Comput. Phys. Commun.* **27**, 229–242.

REDBURN, D. A. & THOMAS, T. N. (1979). Isolation of synaptosomal fractions from rabbit retina. *J. Neurosci. Methods* **1**, 235–242.

ROGERS, J., MATTHEWS, E. K. & MCKAY, D. B. (1987). Effects of a cytosolic protein on the interaction of rat pancreatic zymogen granules *in vitro*. *Biochim. biophys. Acta* **897**, 217–228.

SALZBERG, B. M. & OBAID, A. L. (1988). Optical studies of the secretory event at vertebrate nerve terminals. *J. exp. Biol.* **139**, 195–231.

SALZBERG, B. M., OBAID, A. L. & GAINER, H. (1985). Large and rapid changes in light scattering accompany secretion by nerve terminals in the mammalian neurohypophysis. *J. gen. Physiol.* **86**, 395–411.

SALZBERG, B. M., OBAID, A. L., GAINER, H. & SENSEMAN, D. M. (1983). Optical recording of action potentials from vertebrate nerve terminals using potentiometric probes provides evidence for sodium and calcium components. *Nature, Lond.* **306**, 36–40.

SATTELLE, D. B., GREEN, D. J. & LANGLEY, K. H. (1975). Laser light scattering from a neurosecretory tissue. *Biol. Bull. mar. biol. Lab., Woods Hole* **149**, 455.

SATTELLE, D. B., GREEN, D. J., LANGLEY, K. H. & WESTHEAD, E. W. (1976). Size and dispersity of isolated secretory (chromaffin) granules. *Biol. Bull. mar. biol. Lab., Woods Hole* **151**, 428–429.

SATTELLE, D. B., LANGLEY, K. H., OBAID, A. L. & SALZBERG, B. M. (1987). Laser light scattering determination of size and dispersity of synaptosomes and synaptic vesicles isolated from squid (*Loligo pealei*) optic lobes. *Eur. Biophys. J.* **15**, 71–76.

SATTELLE, D. B., LEE, W. I. & WARE, B. R. (1982). (ed.) *Biomedical Applications of Laser Light Scattering*. pp.1–427. Amsterdam: Elsevier Biomedical Press.

SATTELLE, D. B. & PIDDINGTON, R. W. (1975). Potassium-induced motion increase in a central nervous ganglion. *J. exp. Biol.* **62**, 753–770.

SHAW, T. I. & NEWBY, B. J. (1972). Movement in a ganglion. *Biochim. biophys. Acta* **255**, 411–412.

SIEGEL, D. P. & WARE, B. R. (1980). Electrokinetic properties of synaptic vesicles and synaptosomal membranes. *Biophys. J.* **30**, 159–171.

SIEGEL, D. P., WARE, B. R., GREEN, D. J. & WESTHEAD, E. W. (1978). The effects of calcium and magnesium on the electrophoretic mobility of chromaffin granules measured by electrophoretic light scattering. *Biophys. J.* **28**, 341–346.

SULLIVAN, R. E., FRIEND, B. J. & BARKER, D. L. (1977). Structure and function of spiny lobster ligamental nerve plexuses: evidence for synthesis, storage, and secretion of biogenic amines. *J. Neurobiol.* **8**, 581–605.

WARE, B. R. & FLYGARE, W. H. (1971). The simultaneous measurement of the electrophoretic mobility and diffusion coefficient in bovine serum albumin solutions by light scattering. *Chem. Phys. Letts* **12**, 81–85.